

Test of elaboration protocols for obtaining highly Co- or Ni -alloyed spheroidal cast irons from an industrial SG cast iron. Part C: Second protocol for 25M75Fe cast irons. Subpart 1: Obtained microstructures and room temperature hardness

Kamel Meridja, Patrice Berthod*, Elodie Conrath

Institut Jean Lamour (UMR 7198), Team 206 "Surface and Interface, Chemical Reactivity of Materials" Faculty of Sciences and Technologies, University of Lorraine, B.P. 70239, 54506 Vandoeuvre-lès-Nancy, (FRANCE)
E-mail: Patrice.Berthod@univ-lorraine.fr

ABSTRACT

Spheroidal Graphite cast irons highly alloyed with nickel or with cobalt were produced by foundry from parts of an industrial SG cast iron, by following a protocol which recently proved its efficiency, despite that no additional spheroidisation and inoculation treatments of the liquid metal was done. The same protocol was applied to obtain a control sample containing only iron. For the obtained 25wt.%Ni- and 25wt.%Co-containing cast irons the graphite issued from this protocol is very close to the spheroidal geometry. Obtaining highly alloyed SG cast iron following this original elaboration route was thus successful. The matrix of the obtained 25wt.%Ni- and 25wt.%Co-containing cast alloys was influenced by the presence of these new elements in so high quantities: absence of the hypoeutectic character of the control sample, respectively metallic matrix or ferrite-pearlitic matrix instead the ledeburite of the control sample. Graphitizing properties were found again for nickel and revealed for cobalt. The differences of Vickers hardness between the three cast irons were easily explained and hypothesis were formulated, from the response of the microstructures to the Nital etching, about the corrosion resistance of these two highly alloyed SG cast irons.

© 2016 Trade Science Inc. - INDIA

KEYWORDS

Spheroidal graphite cast iron;
Nickel;
Cobalt;
Microstructure;
Optical microscopy;
SEM.

INTRODUCTION

Cast irons may be simple Fe-Si-C alloys containing only traces of other elements^[1, 2] or they can be alloyed with several elements simultaneously (e.g. Ni, Co, Mo, Ti...) whose contents may be of around 1 wt.% each^[3]. They can be also alloyed specifi-

cally with Cr and Ni^[4] or only Ni^[5, 6] for a better corrosion resistance or better mechanical properties^[7]. Cobalt can be also present in the chemical composition of cast irons, simultaneously with Ni^[8,9] or not. Some grey cast irons (with flake graphite or spheroidal graphite), highly alloyed to nickel contain about 20-25wt.%Ni, already exist, but often with

Full Paper

presence of other elements than Fe, Si, C and Ni. Similar cast irons, with cobalt instead nickel in the same contents, are rarer. In this work we were interested by spheroidal graphite cast irons, only containing Fe, Si, C and either Ni or Co, with 25wt.% in both cases. In this first part we describe how we elaborate them and the microstructures that have the obtained ingots. In a second part we will present the mechanical properties of these 25wt.%Ni or 25wt.%Co-containing cast irons.

EXPERIMENTAL

Elaboration of the alloys

The alloys of interest in this work were elaborated following the procedure which recently led more to spheroidal graphite than in the first elaborations that we did involving the re-melting of industrial SG cast iron^[9]. The route was then the same as the one followed in^[10]. First a part of the same spheroidal graphite cast iron ingot as in^[9, 10] (industrial origin) was cut (weight about 30g). This industrial ingot contains about 3.5 wt.%C and 2.5 wt.%Si. To respect these carbon and silicon contents supplementary 10 grams of new charge was prepared from pure elements: M, C and Si, with M being either Co or Ni. The targeted C and Si contents for these new 10g of additional alloy were the same as the one of the industrial ingot. These 10g were melted in the water-cooled copper crucible of a CELES furnace, under about 400 mbars of pure Argon, following the thermal cycle described thereafter: 1 minute at 2.5 kV, increase in voltage up to more than 5kV and dwell at this voltage until the main part of graphite was really incorporated in the molten alloy. In a second step, the 10 grams of obtained alloy were melted together with the 30g of industrial SG iron, following a thermal cycle allowing total melting but also respecting the conditions of spheroidal shape conservation for graphite by limiting overheating: 30 seconds stage at 2.5kV, then 30 seconds only at 3.5kV and rapid cooling.

Here too a third alloy was added for comparison, combining 30g of industrial SG cast iron and 10g of synthetic Fe-3.5C-2.5Si, elaborated follow-

ing the same two-steps route described just before.

Ingots' cutting and samples' machining

The obtained ingots were first immersed in a liquid mix of cold resin system (82% CY230 resin and 18% HY253Hardener closely mixed together) in order to obtain a cylindrical mounted ingot much easier to handle, then cut using a Buehler Abrasimet Delta metallographic saw. Parts for the metallographic characterization and parallelepipeds devoted to the compression tests were thus obtained.

Metallographic characterization

The parts prepared for the metallographic observations were imbedded in the same cold resin system as mentioned above, ground with SiC papers (grade increasing from 120 to 4000). They were ultrasonically cleaned, then polished using a textile disk supplied in 1µm alumina particles.

The mounted and polished samples were observed by optical microscopy. A Olympus optical microscope (BX51 model) equipped with a digital camera (ToupCam) driven with a software (ToupView), was used to examine the shape of the obtained graphite. Thereafter they were etched by Nital (ethanol-4% HNO₃) during a 10s-immersion at room temperature, to allow the observation of the metallic matrix (same optical microscope). The image analysis tool of the Adobe Photoshop CS of Adobe was used for measuring the surface fractions of graphite.

The samples were also observed by electron microscopy, using a Scanning Electron Microscope (SEM) JEOL JSM 6010LA. This one was equipped with an Energy Dispersion Spectrometry (EDS) device which was employed for controlling the global chemical compositions of the obtained ingots and to measure the chemical composition of the matrix.

Estimation of the density and indentation tests

The parts devoted to the compression test^[11] were accurately weighed (microbalance, precision ±0.1mg) and their dimensions measured using an electronic calliper. The mass/volume ratio was calculated to estimate the densities of the three 25M-75FGS cast alloys.

The Vickers hardness of the alloys was measured

on the metallographic samples. This was done by applying a 10kg load during 10 seconds with a Testwell Wolpert machine equipped with a pyramidal diamond indentor.

RESULTS AND DISCUSSION

Optical microstructure observations

The obtained microstructures are illustrated by optical microphotos in Figure 1 (SEM/Back Scattered Electron mode) and in Figures 2-4 (optical microscope, microstructures after etching by Nital). The obtained shape of graphite is globally spheroidal in the “25Ni75FGS” and “25Co75FGS” cast irons, even it seems degenerated (Figure 1).

In contrast graphite is rather rare in the “25Fe75FGS” cast iron, but the particles seem being very spheroidal. Image analysis measurements show that there are globally the same surface fractions of graphite in the 25Co75FGS and 25Ni75FGS cast irons while the one in 25Fe75FGS is about ten

times lower (TABLE 1).

After etching the matrix of the 25Ni75FGS cast iron appears (Figure 2). This one seems globally metallic. However one can see some zones, along the periphery of the eutectic cells, which are coloured in yellow/orange: may be traces of pearlite.

After Nital etching the 25Co75FGS cast iron appears as clearly ferrito-pearlitic (Figure 3). Its matrix is composed of a shell of ferrite (white) surrounding the graphite nodules (black), and of pearlite (grey).

In contrast, Nital etching shows that the microstructure of the 25Fe75FGS is totally different (Figure 4). Indeed many plates of cementite (Fe_3C), appearing white, are present, mixed with elongated areas of pearlite. There is a rather dense network of grey dendrites. These ones precipitated early during solidification (pre-eutectic part of solidification) before that the residual interdendritic liquid crystallizes in mainly ledeburite. This white eutectic Fe-C compound, made of plates of eutectic austenite

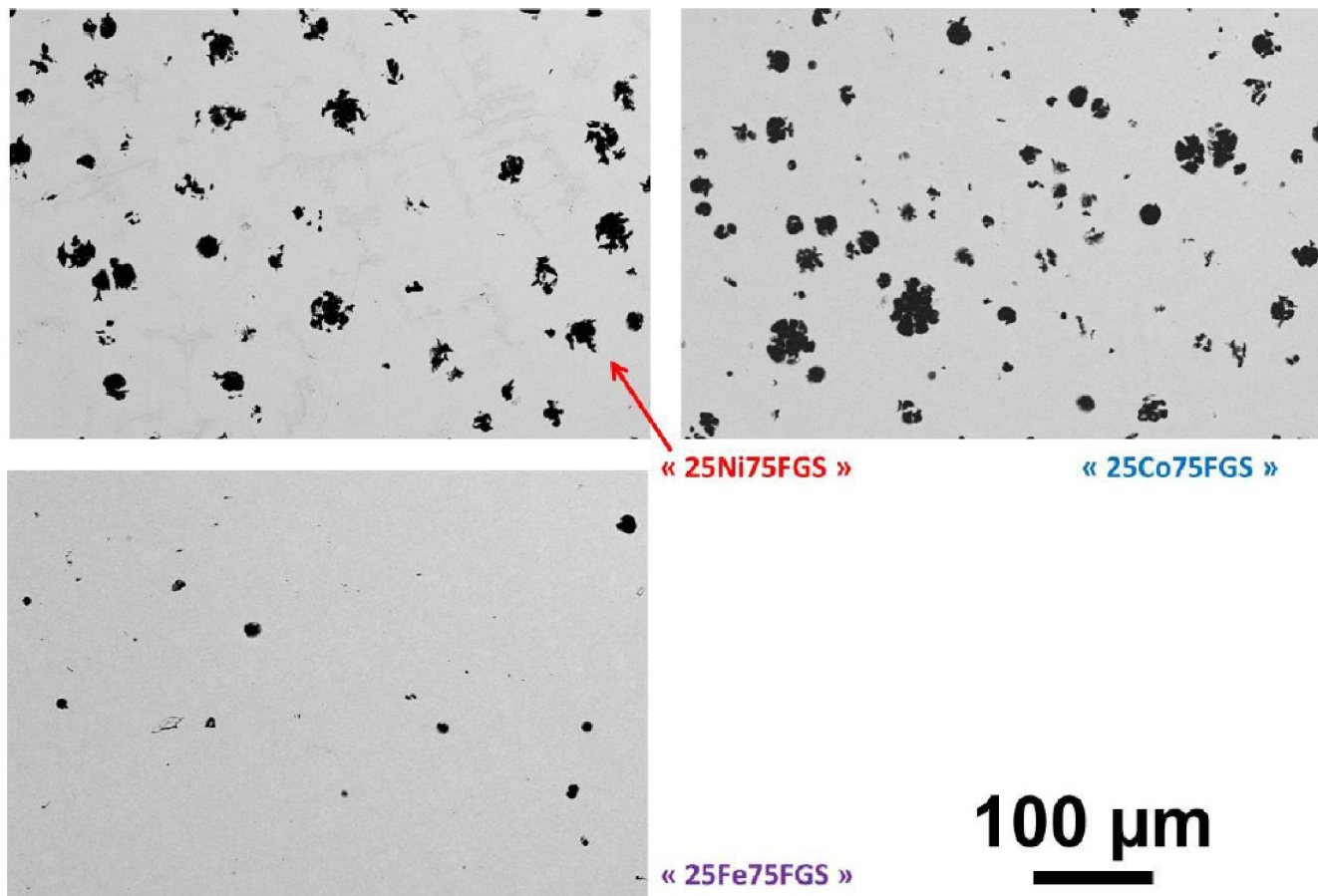


Figure 1 : Visualisation of graphite by SEM/BSE observation before nital etching

Full Paper

TABLE 1 : Results of graphite surface fractions as measured by image analysis

Alloys	Surface fraction of graphite (%)
« 25Co75FGS »	6.41
« 25Ni75FGS »	5.19
« 25Fe75FGS »	0.56

and of plates of cementite, with lateral growth of austenite fibres in a matrix or cementite, was predominant, even if some small graphite nodules are also present (not easily visible after Nital etching but better seen before etching in Figure 1). The austenite thereafter transformed into pearlite at the eutectoid temperature, this solid state transformation leading to the pearlite (dendrites and plates&fibres in ledeburite).

SEM/EDS characterization

The observations carried out with the SEM did not give additional information about the as-cast microstructures of the three cast irons. The EDS allowed controlling the chemical compositions and showed that the targeted contents in Ni and in Co notably were globally well respected (TABLE 2).

The chemical composition of the matrix was also analysed (TABLE 3). The results show that the Co and Si local contents in the matrix of the 25Co75FGS cast iron are not homogeneous. There are zones type 1 which are rich in cobalt and in silicon (about 26 wt.% Co-2.7wt.% Si) and zones type 2 poor in these

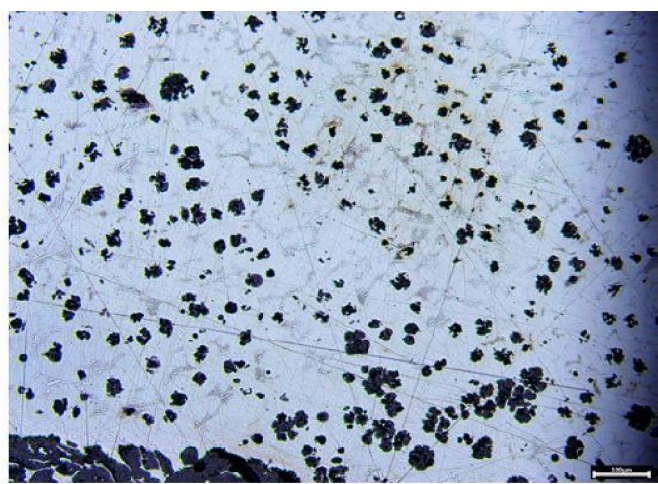
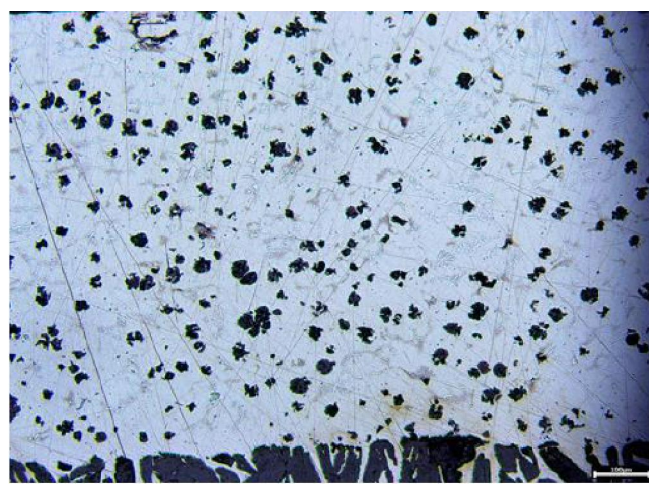
two elements (about 19 wt.% Co-less than 1wt.% Si). One can guess that the zones of type 1 are the shell surrounding the nodules (ferrite, promoted by Si) and the zones of type 2 are the zones which are farer from the nodules (pearlite, usually very poor in Si).

There are similar zones in the 25Ni75FGS cast iron, of type 1 (rich in Ni: about 22 wt.% and in Si: 2.4wt.%) and of type 2 (poor in Ni and in Si). One can point out that, since it was not so easy to observe the microstructure with the SEM as with the optical microscope after Nital etching, the different spot analyses, the results of which led to the average and standard deviation values, were not rigorously done in the vised parts of the microstructures. This explains the rather scattered results and then the great values of standard deviations for the less extended areas (pearlite).

There are also types of microstructural zones in the 25Fe75FGS cast iron, a first one richer in Si than the second one. They are probably the pearlite (richer in silicon because involving a significant part of ferrite) and ledeburite zones (rich in cementite poor in Si), respectively.

Density and hardness

The values of volume mass and the hardness of the three cast irons are displayed in TABLE 4. The 25Co75FGS seems denser than the two other cast irons. The hardness of the 25Ni75FGS cast iron is



25Ni75FGS

250 μm

Figure 2 : Matrix structure (after nital etching) of the 25Ni75FGS cast iron as observed in three locations

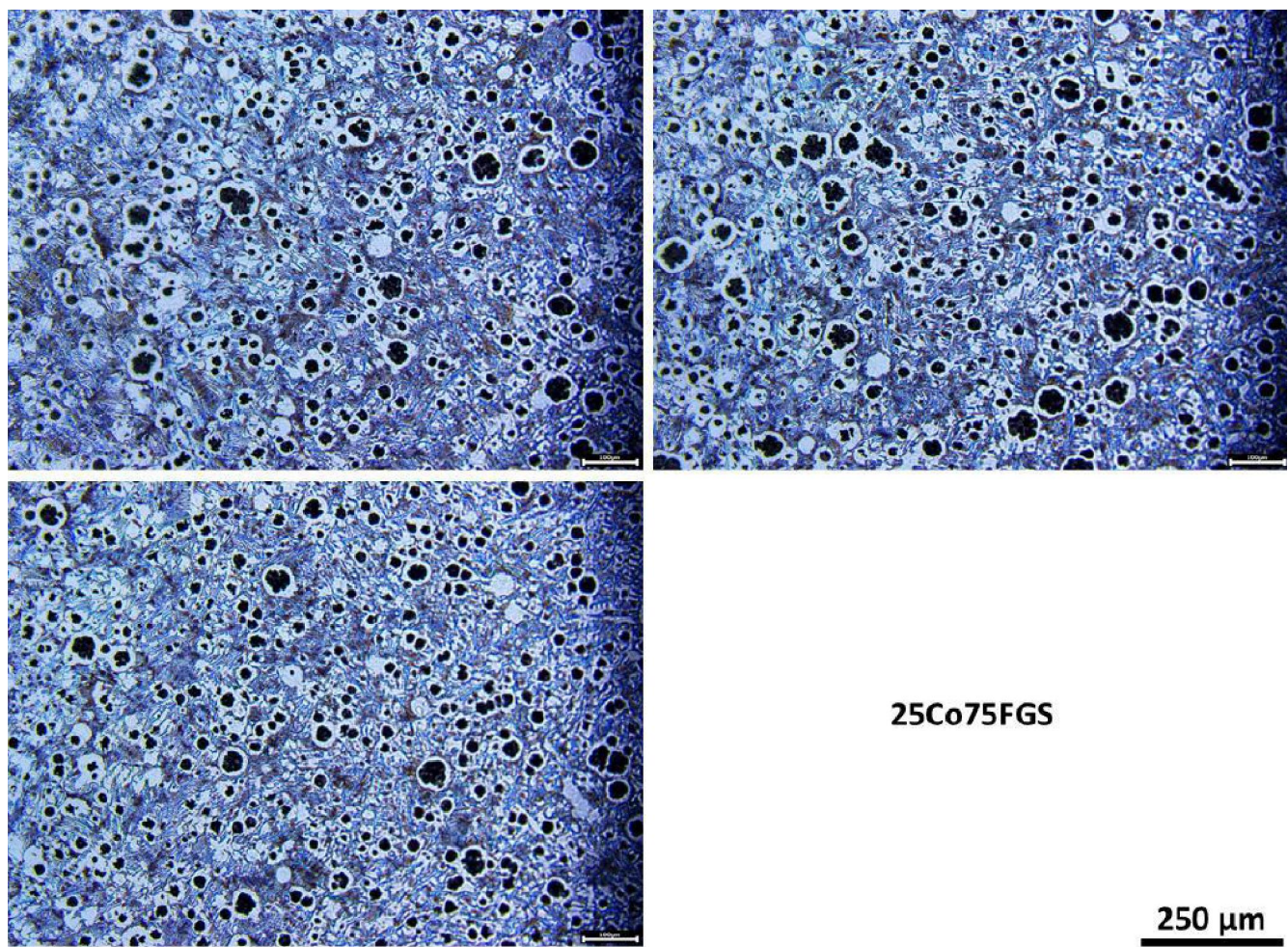


Figure 3 : Matrix structure (after Nital etching) of the 25Co75FGS cast iron as observed in three locations

only half the ones of the 25Co75FGS and 25Fe75FGS cast irons.

General commentaries

The first remarks to do concern the type of graphite which was obtained. Globally the 25wt.%Ni-containing cast iron (25M75FGS) presents graphite particles which are not perfectly spheroidal but with a geometry much closer to spheroids than a 50Ni50FGS recently elaborated^[10] following the same route (two steps fusion) and respecting the same parameters (power and duration of the two isothermal stages, cooling rate). It seems clear that when the wished nickel content increases (up to 50wt.% for the metallic part of the chemical composition) the nodularity of graphite decreases (no Ni: spheroids, 25wt.% Ni: spheroids a little deteriorated, 50wt.%Ni: lamellae and plates). The nature of the nickel phase is also dependent on the Ni content (no

Ni: ledeburite, 25wt.% Ni: pearlite in the zone being the most far from nodules, 50wt.%Ni: matrix totally metallic, no carbides).

Concerning cobalt, the 25wt.%Co-containing cast iron presents itself a graphite with a shape not perfectly spheroidal but much close to the nodular shape than for the 50Co50FGS recently studied^[10]. One can here too resume the effect of cobalt alloying on the graphite morphology, by: no Co: spheroids, 25wt.% Co: spheroids a little deteriorated, 50wt.%Co: deteriorated nodules and lamellae). Although elaborated strictly identically to what was done here, the latter one contained some graphite particles looking like spheroids but mainly lamellae. Similarly to what was observed for the nickel alloys the matrix continuously varies with the Co content: no Co: ledeburite, 25wt.% Co: ferrite-pearlitic “bull’s eyes” matrix, 50wt.%Co: totally metallic matrix).

Concerning the 25Fe75FGS, especially elabo-

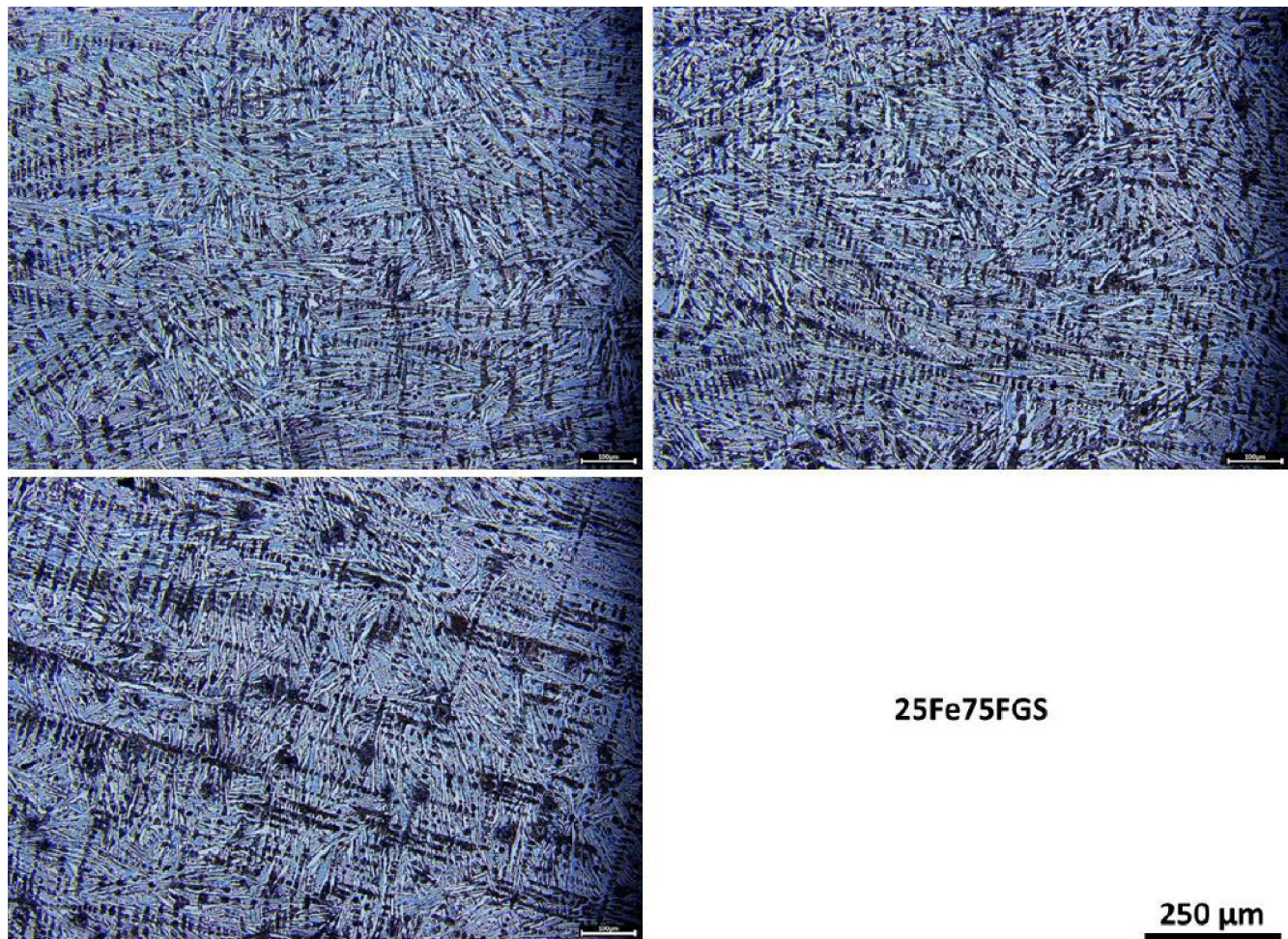


Figure 4 : Matrix structure (after Nital etching) of the 25Fe75FGS cast iron as observed in three locations

TABLE 2 : Global chemical compositions of the « 25M75Fe » alloys (SEM/EDS) ; C cannot be analyzed by EDS

Alloy	Protocol 2	Ni	Co	Fe	Si	C
« 25Co75FGS »		/	24.5 ± 0.7	73.3 ± 0.8	2.2 ± 0.1	not analyzed
« 25Ni75FGS »		22.6 ± 0.3	/	75.2 ± 0.5	2.3 ± 0.3	not analyzed
« 25Fe75FGS »		/	/	97.7 ± 0.1	2.3 ± 0.1	not analyzed

rated to be able to compare the specific effects of Ni and Co, it appears that the microstructure looks like the one of the 50Fe50FGS alloy earlier studied (dendrites of austenite transformed in pearlite, ledeburite, an nodular iron; however there is a little difference with the 50Fe50FGS: nodules seems being less numerous than in the 50Fe50FGS, despite the fact that the nucleus are two times less diluted in the present case. The particularly low surface fraction of graphite is due to the high quantity of carbon involved in the cementite part of ledeburite.

Besides the graphite morphology, the comparison between the 25Ni75FGS and the 25Fe75FGS

reveals that 25wt.% of Ni lead to much less carbides, and also maybe to a eutectic (even hypereutectic?) nature of cast iron, while the 25Fe75FGS was clearly hypo-eutectic (obvious presence of pre-eutectic dendrites). The same effects are observed for 25wt.%Co. Logically, the 3.5wt.%C associated with the 2.5 wt.%Si, lead to an equivalent carbon content of 3.5 wt.% + (2.5wt.% / 3) = 4.33 wt.%, equal to the eutectic value. If the control sample 25Fe75FGS cast iron contains dendrites this is because of the delay at solidification due to the passage from the stable austenite-graphite phase diagram to the metastable austenite-cementite one. In

TABLE 3 : Matrix chemical compositions of the « 25M75Fe » alloys (SEM/EDS); C cannot be analyzed by EDS

Alloy	Protocol 2	Ni	Co	Fe	Si	C
« 25Co75FGS »	Type zone 1	/	25.8 ±0.7	70.6 ±1.4	2.7 ±0.4	<i>not analyzed</i>
	Type zone 2	/	19.2 ±0.7	80.2 ±1.2	0.6 ±0.6	
« 25Ni75FGS »	Type zone 1	21.9 ±0.3	/	75.7 ±0.5	2.4 ±0.1	<i>not analyzed</i>
	Type zone 2	16.5 ±7.1	/	72.2 ±7.1	1.4 ±0.8	
« 25Fe75FGS »	Type zone 1	/	/	97.3 ±0.4	2.7 ±0.4	<i>not analyzed</i>
	Type zone 2	/	/	89.5 ±1.4	1.7 ±0.3	

TABLE 4 : Density and hardness of the obtained alloys

Alloys	Density	Hardness
« 25Co75FGS »	7.22 g/cm ³	159 ±5
« 25Ni75FGS »	6.06 g/cm ³	77 ±6
« 25Fe75FGS »	6.37 g/cm ³	157 ±7

the case of the 25Ni75FGS cast iron the matrix is not attacked by Nital and it is true that dendrites are particularly visible when austenite is transformed into pearlite (grey after Nital etching). In contrast, Nital etching was much more efficient for the 25Co75FGS cast iron and no dendrites were revealed in its case. Considering that these two alloys are well eutectic and that solidification obviously took place according to the stable phase diagram (austenite-graphite) as demonstrated by the absence of ledeburite and the presence of coarse graphite semi-nodules, it is clear that, for equivalent cooling rates, the 25wt.% of Ni or of Co led to a solidification integrally in the stable diagram : the graphitizing character of nickel was already well known but the one of cobalt may be less. In contrast the effects of nickel and of cobalt concerning the eutectoid transformation are not the same. One can logically think that the matrix of the as-cast 25Ni75FGS cast iron is austenitic rather than ferritic: no grain boundaries were seen after Nital etching.

Concerning the hardness, the differences are easily explainable: the 25Ni75FGS with its matrix totally free of carbides is logically less hard than the two other cast irons which contain carbides. However one can point out that the 25Co75FGS is globally as hard as the 25Fe75FGS one, despite that the first one contains only pearlite while the second one contains ledeburite. One can expect a 25Fe75FGS75 significantly harder than the 25Co75FGS, but the presence of so high Co content

maybe leads to harder ferrite and pearlite.

To finish one can also highlighting that the absence of response of the 25Ni75FGS to Nital etching, by comparison with the two studied cast irons, suggests that the 25Ni75FGS cast iron is much more resistant against corrosion than the two other alloys. Despite that the duration of exposure to Nital was extremely short (only 10 seconds) one can guess that the corrosion behaviour of this nickel-alloyed cast iron is much better than the other cast irons' ones.

CONCLUSION

The second protocol of elaboration recently defined for obtaining Ni-alloyed and Co-alloyed Spheroidal Graphite cast irons from industrial SG cast irons and without any treatment of the liquid metal was obviously efficient – but not perfect – for obtaining cast irons highly alloyed to either Ni or Co (25wt.%) by preserving a good part of the initial graphite geometry. Some interesting observations concerning the effect of these elements on the matrix nature, on the consequences of hardness, and on the character of the cast irons by regards to the eutectic were also done. Now these 25wt.% Ni- or 25wt.%Co-containing SG cast irons will be studied by mechanical tests^[11].

REFERENCES

- [1] J.R.Davis; Cast Irons, ASM International, (1996).
- [2] M.Durand-Charre; Microstructure of steels and cast irons – Engineering materials and processes, Springer-Verlag, Berlin Heidelberg New York, (2004).
- [3] M.Wojtasik, T.Rybka, E.Wojciechowski, R.Zawodny; Patent, PL1977-198604, (1977).
- [4] A.A.Tahirov, N.S.Gushchin; Liteinoe Proizvodstvo, 12, 2 (2012).

Full Paper

- [5] Y.Z.Liu, L.L.Sun, C.A.Li, J.Xiong, Y.F.Wang; Zhongnan Daxue Xuebao, Ziran Kexueban, **43(10)**, 3832 (**2012**).
[6] J.C.Morrison; Giesserei-Praxis, **12**, 483 (**1998**).
[7] C.Zhou; Patent, CN 2015-10341175, (**2015**).
[8] X.Hu, Z.Wang, K.Huang, F.Li, P.Li; Patent, CN 2010-10177246, (**2010**).
[9] K.Meridja, P.Berthod, E.Conrath; Materials Science : An Indian Journal, **14(4)**, 130 (**2016**).
[10] K.Meridja, P.Berthod, E.Conrath; Materials Science : An Indian Journal, **14(4)**, 139 (**2016**).